NOVEL WAVE EFFECTS ON ANISOTROPIC AND FERRITE PLANAR SLAB WAVEGUIDES IN CONNECTION WITH SINGULARITY THEORY

Alexander B. Yakovlev[1] and George W. Hanson[2]

[1]Department of Electrical Engineering, The University of Mississippi, University, Mississippi, 38677, USA
[2]Department of Electrical Engineering and Computer Science, University of Wisconsin-Milwaukee, Milwaukee, Wisconsin, 53211, USA

Abstract— **The characteristic interactions of discrete modes supported by planar isotropic and anisotropic dielectric and ferrite slab waveguides are analyzed using singularity and critical point theory, leading to a rigorous and complete explanation of all modal interactions. For an anisotropic planar waveguide having an arbitrarily-orientated optical axis, it is shown that mode coupling is controlled by the presence of an isolated Morse critical point accompanied by a pair of complex-conjugate frequency-plane branch points. The interaction of space-wave leaky modes on a grounded anisotropic slab is studied by investigating the evolution of complex frequency-plane branch point singularities as the orientation of the optical axis varies. Space-wave leaky modes of a biased grounded ferrite slab waveguide are studied in connection with different types of branch-point singularities, resulting in the observation of novel wave effects on ferrite slabs. The general theory is presented, and numerical results are provided for some specific waveguides.**

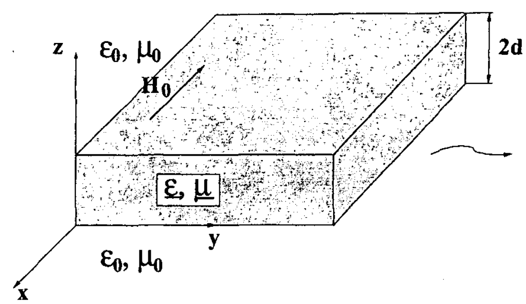

Fig. 1. A complex-media planar slab waveguide.

I. Introduction

Dielectric waveguides are often fabricated using isotropic dielectrics, although anisotropic dielectrics may be incorporated either intentionally or unintentionally. Naturally occurring anisotropic materials may be intentionally chosen as a waveguide material for a variety of reasons, such as to enhance polarization-based effects [1]. In addition, waveguide materials may exhibit processing-induced anisotropy, such as often occurs in forming planar layers for circuit boards [2]. Anisotropy can have a significant effect on modal coupling and cutoff properties, and must often be accounted for in electromagnetic simulations for design and analysis of guided-wave structures and devices. In particular, the presence of anisotropy can induce mode coupling in a waveguiding structure that would not admit such coupling when constructed using isotropic materials [3], [4]. Biased ferrites with anisotropic permeability are used in various nonreciprocal devices such as phase shifters, polarizers, and isolators, where electromagnetic properties of such devices are controlled by varying the applied magnetic bias field [5]–[7].

Unfortunately, the dispersion characteristics of all but the simplest waveguiding structures (e.g., homogeneously-filled parallel conducting plates or closed rectangular waveguides) must be determined numerically, which obscures the analytical character of the dispersion function. In recent papers we have presented a method based on singularities and critical points which helps to reveal the analytical character of the dispersion function and explain observable modal phenomena. In [8] singular points and associated frequency-plane branch points were shown to govern modal behavior in the vicinity of cutoff in a variety of transmission line and waveguiding structures. In [9] Morse critical points were shown to provide an alternative to traditional coupled-mode theory for general transmission lines and waveguides. In [10] the TM-even modes supported by an isotropic planar waveguide were studied, and complex frequency-plane branch points associated with these modes were identified. This lead to an explanation of the "apparent" modal nonuniqueness of TM-even surface-wave modes supported by a planar waveguide having material loss or gain. In [11] it was shown that branch points are also associated with Morse critical points which occur in mode coupling regions, such that mode interactions will have the form of either mode transformations or mode continuations, depending on the path of frequency variation with respect to the location of the frequency-plane branch points.

0-7803-7239-5/02/$10.00 © 2002 IEEE

In this work we apply the theory of singular and critical points to explain modal phenomena on anisotropic planar dielectric waveguides, making use of the isotropic waveguide results, and investigate discrete forward, backward, and associated space-wave leaky modes on biased ferrite slabs in connection with singularity theory.

II. Singularities and Critical Points of the Dispersion Function

Considering the two-dimensional complex-media planar waveguiding structure depicted in Figure 1, which is invariant along the waveguiding ρ-axis ($\rho = \sqrt{x^2+y^2}$), and subsequent to a two-dimensional Fourier transform in space and time, $(\rho, t) \longleftrightarrow (\lambda, \omega)$, source-free Maxwell's equations can be converted to an operator equation for the discrete modes of the structure,

$$A\left(\lambda, \omega, \underline{\varepsilon}, \underline{\mu}, d\right) X = 0. \qquad (1)$$

In general, a planar slab waveguide shown in Figure 1 represents a planar bianisotropic medium, but in this paper we are considering two separate cases of anisotropic slab with the permittivity tensor $\underline{\varepsilon}$ and $\underline{\mu} \equiv \mu_0$ and ferrite slab with the permeability tensor $\underline{\mu}$ and $\underline{\varepsilon} \equiv \epsilon_0 \epsilon_r$. In (1) A is an operator-function, λ is the spatial Fourier-transform variable representing the modal propagation constant (note that λ is a radial transform variable, and not wavelength), ω is the temporal Fourier-transform variable representing angular frequency, and X represents a modal field distribution, typically current density, electric field, or magnetic field, depending on the problem formulation. We consider the analytic continuation of each of the variables (λ, ω) into the complex plane, and assume that $\underline{\varepsilon}$, $\underline{\mu}$, and d have specified values. The dyadic permittivity $\underline{\varepsilon}$ is given by

$$\underline{\varepsilon} = R^T(\theta, \phi) \begin{bmatrix} \varepsilon_{xx} & 0 & 0 \\ 0 & \varepsilon_{yy} & 0 \\ 0 & 0 & \varepsilon_{zz} \end{bmatrix} R(\theta, \phi), \qquad (2)$$

where

$$R(\theta, \phi) = \begin{bmatrix} \cos\theta\cos\phi & \cos\theta\sin\phi & -\sin\theta \\ -\sin\phi & \cos\phi & 0 \\ \sin\theta\cos\phi & \sin\theta\sin\phi & \cos\theta \end{bmatrix} \qquad (3)$$

represents a rotation matrix which fixes the position of the optical axis, and R^T is the transpose of R.

The dyadic permeability $\underline{\mu}$ is given by

$$\underline{\mu} = \mu_0 R(\theta, \phi) \begin{bmatrix} \mu & \jmath\kappa & 0 \\ -\jmath\kappa & \mu & 0 \\ 0 & 0 & 1 \end{bmatrix} R^T(\theta, \phi), \qquad (4)$$

where $\mu = 1 + (\omega_0 \omega_M)/(\omega_0^2 - \omega^2)$, $\kappa = \omega\omega_M/(\omega_0^2 - \omega^2)$, $\omega_0 = \gamma\mu_0 H_0$, $\omega_M = \gamma\mu_0 M_s$, and H_0 is the dc magnetic bias field, M_s is the material saturation magnetization, and $\gamma = -1.759 \times 10^{11}$ kg/coul.

Non-trivial solutions of (1) are obtained from the implicit dispersion equation

$$H\left(\lambda, \omega, \underline{\varepsilon}, \underline{\mu}, d\right) = \det\left(A\left(\lambda, \omega, \underline{\varepsilon}, \underline{\mu}, d\right)\right) = 0. \qquad (5)$$

More generally, H is a mapping $\left(\lambda, \omega, \underline{\varepsilon}, \underline{\mu}, d\right) \rightarrow \mathbf{C}$ such that

$$H\left(\lambda, \omega, \underline{\varepsilon}, \underline{\mu}, d\right) = C \qquad (6)$$

where $C \in \mathbf{C}$ is a complex-valued constant in the complex space $\mathbf{C}$, i.e., given $\underline{\varepsilon}$, $\underline{\mu}$, and d only for certain values of (λ, ω) is $C = 0$. By treating (λ, ω) as a pair of complex variables, a study of the properties of the mapping H leads to the analysis of critical points and associated complex frequency-plane branch points which explain modal phenomena. We assume that the mapping H is continuous, and that all second partial derivatives of H exist and are continuous. For a given operator-function this is usually easy to prove.

Since $\underline{\varepsilon}$, $\underline{\mu}$, and d have specified values, the pair of variables (λ, ω) belongs to one of three possible categories. If

$$\frac{\partial H(\lambda,\omega)}{\partial \lambda} = H'_\lambda(\lambda, \omega) = 0, \quad \frac{\partial H(\lambda,\omega)}{\partial \omega} = H'_\omega(\lambda, \omega) = 0 \qquad (7)$$

we call $(\lambda, \omega) = (\lambda_c, \omega_c)$ a *critical point* of the mapping H. If

$$\frac{\partial H(\lambda,\omega)}{\partial \lambda} = H'_\lambda(\lambda, \omega) \neq 0, \quad \frac{\partial H(\lambda,\omega)}{\partial \omega} = H'_\omega(\lambda, \omega) \neq 0 \qquad (8)$$

then $(\lambda, \omega) = (\lambda_r, \omega_r)$ is said to be a *regular point* of the mapping H. If

$$\frac{\partial H(\lambda,\omega)}{\partial \lambda} = H'_\lambda(\lambda, \omega) \neq 0, \quad \frac{\partial H(\lambda,\omega)}{\partial \omega} = H'_\omega(\lambda, \omega) = 0 \qquad (9)$$

or

$$\frac{\partial H(\lambda,\omega)}{\partial \lambda} = H'_\lambda(\lambda, \omega) = 0, \qquad \frac{\partial H(\lambda,\omega)}{\partial \omega} = H'_\omega(\lambda, \omega) \neq 0 \qquad (10)$$

then $(\lambda, \omega) = (\lambda_s, \omega_s)$ is said to be a *singular point* of the mapping H.

Furthermore, if

$$H\left(\lambda, \omega, \underline{\varepsilon}, \underline{\mu}, d\right) = 0 \qquad (11)$$

then $(\lambda, \omega) = (\lambda_0, \omega_0)$ is a solution of (5) leading to modal dispersion behavior. In this case we are usually interested in determining the implicit dispersion function $\lambda_0\left(\omega_0, \underline{\varepsilon}, \underline{\mu}, d\right)$ for the modal propagation constant as a function of frequency. In fact, for any ω_0 one can find a solution λ_0.

Each modal solution point (λ_0, ω_0) of (5) will be either a critical point, a regular point, or a singular point of the mapping H, although, conversely, critical, regular, and singular points of H are not necessarily modal

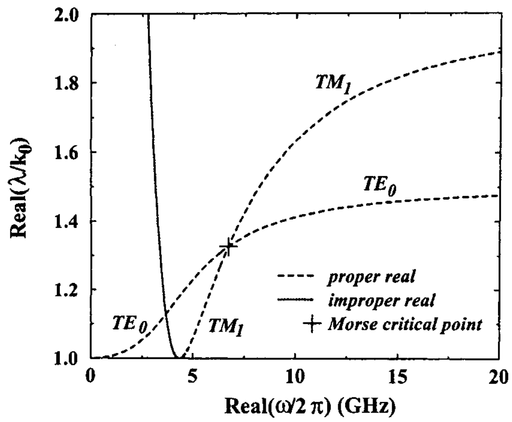

Fig. 2. Dispersion curves for the TM_1 and TE_0 modes when the optical axis is positioned at $\theta = 0°$. The location of a degenerate MCP is shown by the plus sign at the place of intersection of dispersion curves.

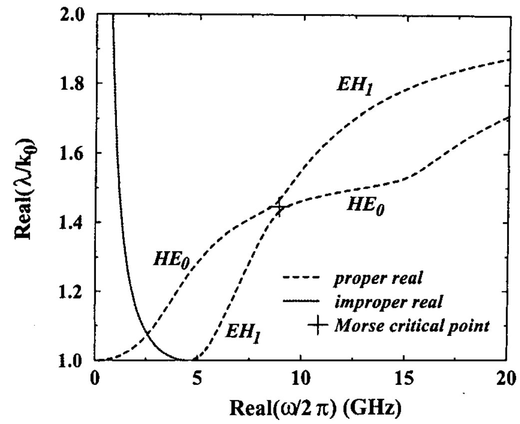

Fig. 3. Dispersion curves for the hybrid EH_1 and HE_0 modes when the optical axis is positioned at $\theta = 45°$ and $\phi = 30°$. The location of the nondegenerate MCP is shown by the plus sign in the region of mode transformation.

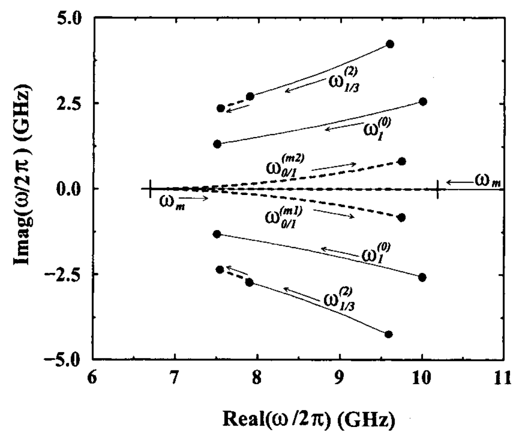

Fig. 4. Migration (parameterized) in the complex frequency plane of various branch points and the MCP associated with the modes shown in Figure 3.

solutions (i.e., they do not necessarily satisfy $H = 0$). From a geometric view, one can consider properties of the surface $\left(\lambda, \omega, \underline{\varepsilon}, \underline{\mu}, d, H\left(\lambda, \omega, \underline{\varepsilon}, \underline{\mu}, d\right)\right)$ in the vicinity of the hyperplane $\left(\lambda, \omega, \underline{\varepsilon}, \underline{\mu}, d, 0\right)$.

III. Singularities Associated with Anisotropic and Ferrite Waveguide Modes

A full-wave solution for a bianisotropic slab waveguide depicted in Figure 1 (anisotropic or ferrite planar slabs considered in this paper) was obtained numerically using the method described in [12]. Dispersion behavior of the TM_1 and TE_0 modes of anisotropic slab with $\theta = 0°$ and $\varepsilon_{xx} = \varepsilon_{yy} = 4\varepsilon_0$, $\varepsilon_{zz} = 2.25\varepsilon_0$, $2d = 2$ cm is shown in Figure 2. In this case ($\theta = 0°$) in the place of the intersection of dispersion curves appears a critical point called a degenerate Morse critical point (MCP), in the sense that $H\left(\lambda_c, \omega_c\right) = 0$, and the dispersion curves form (locally) two intersecting straight lines, indicating that the modes do not couple.

As the optical axis is moved away from a coordinate axis the modes generally become hybrid (although pure TE and TM modes do still exist if the optical axis is moved in certain planes). Dispersion curves of the hybrid EH_1 and HE_0 modes when the optical axis is positioned at $\theta = 45°$ and $\phi = 30°$ is shown in Figure 3. In this case the MCP becomes nondegenerate and in addition two complex-conjugate frequency plane branch points reside symmetrically about the real-ω axis. Since the path of frequency variation passes between these points, mode coupling and associated mode transformation occurs [11].

The migration of the MCP and branch points, as well as the splitting off of the branch points $\omega_{0/1}^{(m1,2)}$ from the MCP as the pure TE and TM modes become hybrid, is shown in Figure 4. The solid lines show migration of the branch points for $\varepsilon_{zz} = 2.25\varepsilon_0$ as $\varepsilon_{xx} = \varepsilon_{yy}$ changes from $2.25\varepsilon_0$ (isotropic case) to $\varepsilon_{xx} = \varepsilon_{yy} = 4\varepsilon_0$ (anisotropic case). The dashed lines show the migration as θ is then changed from 0° to 60° in the plane $\phi = 30°$. As the material becomes anisotropic the MCP moves from infinity to the finite ω-plane (in Figure 4, $\omega_m/2\pi = 6.6921$ GHz for $\varepsilon_{xx} = \varepsilon_{yy} = 4\varepsilon_0$ and $\varepsilon_{zz} = 2.25\varepsilon_0$), and as θ moves away from 0, ω_m migrates as shown (at $\theta = 45°$, $\omega_m/2\pi = 8.904$ GHz and at $\theta = 60°$, $\omega_m/2\pi = 10.179$ GHz) and branch points $\omega_{0/1}^{(m1,2)}$ associated with the nondegenerate MCP emerge (these branch points coalesce at the MCP if θ is brought back to 0).

Numerical results for magnetostatic, TE and TM surface waves, and associated space-wave leaky modes of a

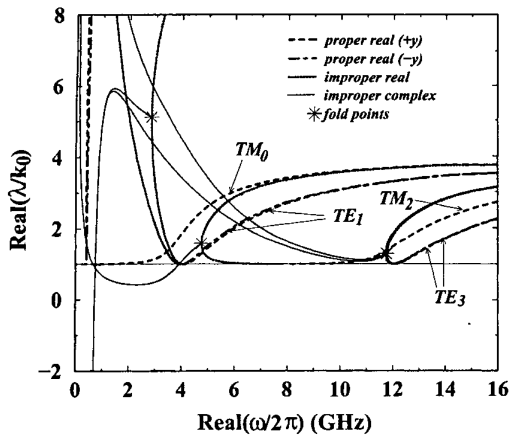

Fig. 5. Dispersion behavior of magnetostatic, TE and TM surface wave modes, and associated space-wave leaky modes of a grounded ferrite slab waveguide having $d = 0.5$ cm, $\epsilon_r = 15$, $H_0 = 10$ G, $\mu_0 M_s = 100$ G.

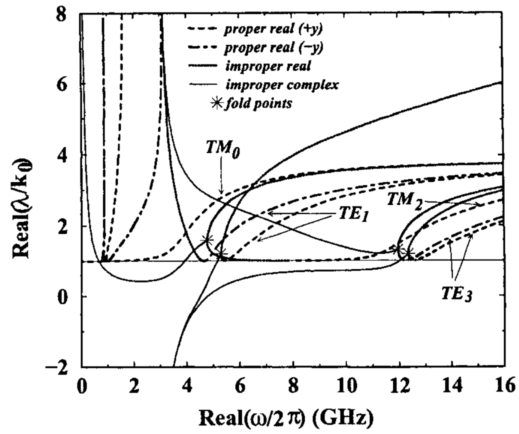

Fig. 6. Dispersion behavior of magnetostatic, TE and TM surface wave modes, and associated space-wave leaky modes of a grounded ferrite slab waveguide having $d = 0.5$ cm, $\epsilon_r = 15$, $H_0 = 100$ G, $\mu_0 M_s = 1000$ G.

grounded ferrite slab waveguide with applied bias magnetic field (Figure 1) are shown in Figures 5 and 6. Starting with the isotropic slab waveguide and identifying various critical and branch point singularities (in particular fold points associated with a leaky wave cutoff), a bias magnetic field was applied resulting in nonreciprocal properties of the slab. With varying bias magnetic field, it occurs that the leaky wave cutoff (for example, of the mode TE_3) splits into two fold points (ω_1 frequency-plane branch points) corresponding to forward and backward surface waves. It was also observed that in a biased grounded ferrite slab the first TE forward mode can possibly leak the energy into free space (Figures 5 and 6) in contrast to isotropic slab waveguides.

IV. Conclusion

In this paper we have presented a general theory which explains modal phenomena in terms of singularities and critical points in the complex frequency plane. As the isotropic material in the waveguide was transformed into an anisotropic and ferrite medium, it was shown that the singularities and critical points associated with the isotropic waveguide migrate in the complex frequency plane. This migration was used to explain modal coupling, modal transformation, and modal interaction phenomena of discrete hybrid surface waves and space-wave leaky modes for the cases of anisotropic and ferrite slab waveguides.

References

[1] K. Kitayama and N. Kumagai, "Theory and applications of coupled optical waveguides involving anisotropic or gyrotropic materials," *IEEE Trans. Microwave Theory Tech.*, Vol. MTT-25, pp. 567–572, July 1977.

[2] N.G. Alexopoulus, "Integrated-circuit structures on anisotropic substrates," *IEEE Trans. Microwave Theory Tech.*, Vol. MTT-33, pp. 847–881, Oct. 1985.

[3] L. Torner, J. Recolons, and J.P. Torres, "Guided-to-leaky mode transformation in uniaxial optical slab waveguides," *IEEE J. Lightwave Technol.*, Vol. 11, pp. 1592–1600, Oct. 1993.

[4] A. Knoesen, T.K. Gaylord, and M.G. Moharam, "Hybrid guided modes in uniaxial dielectric planar waveguides," *IEEE J. Lightwave Technol.*, Vol. 6, pp. 1083–1103, June 1988.

[5] I.Y. Hsia, H.Y. Yang, and N.G. Alexopoulos, "Basic properties of microstrip circuit elements on nonreciprocal substrate-superstrate structures," *J. Electromagn. Waves Applicat.*, Vol. 5, pp. 465–476, 1991.

[6] F. Mesa, R. Marques, and M. Horno, "An efficient numerical spectral domain method to analyze a large class of nonreciprocal planar transmission lines," *IEEE Trans. Microwave Theory Tech.*, Vol. 40, pp. 1630–1640, Aug. 1992.

[7] R. Rafii-El-Idrissi, R. Marques, F. Medina, "Comprehensive analysis of strip- and slot-line guided forward, backward, and complex magnetostatic waves," *IEEE Trans. Microwave Theory Tech.*, Vol. 49, pp. 1599–1606, Sept. 2001.

[8] G.W. Hanson and A.B. Yakovlev, "An analysis of leaky-wave dispersion phenomena in the vicinity of cutoff using complex frequency plane singularities," *Radio Science*, Vol. 33, No. 4, pp. 803–820, July-Aug. 1998.

[9] A.B. Yakovlev and G.W. Hanson, "Analysis of mode coupling on guided-wave structures using Morse critical points," *IEEE Trans. Microwave Theory Tech.*, Vol. 46, pp. 966–974, July 1998.

[10] G.W. Hanson and A.B. Yakovlev, "Investigation of mode interaction on planar dielectric waveguides with loss and gain," *Radio Science*, Vol. 34, No. 6, pp. 1349–1359, Nov.-Dec. 1999.

[11] A.B. Yakovlev and G.W. Hanson, "Mode-transformation and mode-continuation regimes on waveguiding structures," *IEEE Trans. Microwave Theory Tech.*, Vol. 48, pp. 67–75, Jan. 2000.

[12] G.W. Hanson, "A numerical formulation of dyadic Green's functions for planar bianisotropic media with application to printed transmission lines," *IEEE Trans. Microwave Theory Tech.*, Vol. 44, pp. 144–151, Jan. 1996.